Copyright © 2010 Tech Science Press CMES, vol.66, no.2, pp.135-163, 2010

Shape Optimization in Time–Dependent Navier–Stokes Flows via Function Space Parametrization Technique[1]

Zhiming Gao[2] and Yichen Ma[3]

Abstract: Shape optimization technique has an increasing role in fluid dynamics problems governed by distributed parameter systems. In this paper, we present the problem of shape optimization of two dimensional viscous flow governed by the time dependent Navier–Stokes equations. The minimization problem of the viscous dissipated energy was established in the fluid domain. We derive the structure of continuous shape gradient of the cost functional by using the differentiability of a saddle point formulation with a function space parametrization technique. Finally a gradient type algorithm with mesh adaptation and mesh movement strategies is successfully and efficiently applied.

Keywords: shape optimization, shape gradient, gradient type algorithm, time–dependent Navier-Stokes equations, mesh movement.

1 Introduction

A major focus of computational fluid dynamics (CFD) research in the past few years has been on simulating the time dependent behavior of viscous flows. Shape optimization problems for time–dependent Navier–Stokes flows are of great importance in CFD for airplanes, cars, turbines, automotive vehicles, and arterial grafts in biomedical engineering.

Most of the work done in optimization of Navier–Stokes flow has focused on optimal control and steady flows. For instance, Gunzburger (2003) published the book about flow control and optimization; O.Pironneau in Mohammadi and Pironneau

[1] This work is supported by the National Natural Science Fund of China under grant number 11001025.

[2] Corresponding author. Laboratory of Computational Physics, Institute of Applied Physics and Computational Mathematics, P. O. Box 8009-26, Beijing, P. R. China, 100088. E–mail:gao@iapcm.ac.cn.

[3] School of Science, Xi'an Jiaotong University, Shaanxi, P.R.China, 710049. E-mail: ycma@mail.xjtu.edu.cn.

(2001); Pironneau (1984, 1988) computes the derivative of the cost functional using normal variation approach; Murat and Simon (1974) use the formal calculus to deduce an expression for the derivative; J.A.Bello *et.al.* in Bello, Fernandez-Cara, and Simon (1992a,b); Bello, Fernandez-Cara, Lemoine, and Simon (1997) considered this problem theoretically in the case of steady Navier–Stokes flow by the formal calculus; Srinath and Mittal (2007) proposed and implemented a gradient-based procedure based on a continuous adjoint approach for steady low Reynolds number flows (Re=25).

Recently, there has been growing interest in extending optimal design capabilities to unsteady flows. For instance, E.Katamine, H.Azegami, and Y.Matsuura (2003) is concerned with shape identification of unsteady heat conduction fields by the so-called traction method; He, Ghattas, and Antaki (1997) showed the method of shape optimality based on the Bezier curves; Yagi and Kawahara (2005, 2007) investigated the solid body in time–dependent Navier–Stokes flow based on optimal control theory; Abraham, Behr, and Heinkenschloss (2005) carried out shape optimization in the context of non-Newtonian fluids using stabilized finite element methods.

Our concern in this paper is on shape optimization of a body subjected to the minimum dissipation energy in time–dependent Navier–Stokes flows, and on proposing an efficient algorithm for solution of two dimensional realizations of such problems.

For the study of the shape gradient of the cost functional, we will use the so-called function space parametrization technique which was advocated by M.C.Delfour and J.-P.Zolésio to solving Poisson equation with Dirichlet and Nuemann condition (see Delfour and Zolesio (2002)). In our paper Gao and Ma (2006); Gao, Ma, and Zhuang (2008a); Gao and Ma (2008); Gao, Ma, and Zhuang (2008b), we apply them to solve a Robin problem and shape optimization for Stokes and steady Navier–Stokes flow.

In this paper we extend them to study the energy minimization problem for time–dependent Navier–Stokes flow with velocity–pressure boundary conditions in spite of its lack of rigorous mathematical justification in case where the Lagrange formulation is not convex. We shall show how this theorem allows, at least formally to bypass the study of material derivative and obtain the expression of shape gradient for the dissipated energy functional.

One of the major difficulties in shape optimization for time–dependent Navier–Stokes flows is the large number of equality constraints arsing in the time and spatial discretization of the flow state systems.This makes our time–dependent optimization problem in the category of very large scale, nonlinear constrained optimization problem. A gradient type algorithm with mesh adaptation technique and mesh movement strategy is utilized in the present work. Finally, we give some numerical tests concerning on optimization of a two dimensional obstacle located in the time–dependent viscous flow.

This paper is organized as follows. In section 2, we briefly recall the velocity method which is used for the characterization of the deformation of the shape of the domain and give the description of the shape minimization problem for the time–dependent Navier–Stokes flow.

Section 3 is devoted to the computation of the shape gradient of the Lagrangian functional due to a minimax principle concerning the differentiability of the minimax formulation by function space parametrization technique.

Finally in section 4, we give its spatial and time discretization and propose a gradient type algorithm with some numerical examples.

2 Preliminaries and statement of the problem

2.1 Elements of the velocity method

To our little knowledge, there are about three types of techniques to perform the domain deformation: Hadamard (1907)'s normal variation method, the perturbation of the identity method by Simon (1980) and the velocity method (see Céa (1981) and Delfour and Zolesio (2002); Zolesio (1979)). We will use the velocity method which contains the others. In that purpose, we choose an open set D in $\mathbb{R}^N$ with the boundary ∂D piecewise C^k, and a velocity space $\mathrm{E}^k := \{V \in C([0,\varepsilon];\mathscr{D}^k(\bar{D},\mathbb{R}^N)) : V\cdot n_{\partial D} = 0 \text{ on } \partial D\}$, where ε is a small positive real number and $\mathscr{D}^k(\bar{D},\mathbb{R}^N)$ denotes the space of all $k-$times continuous differentiable functions with compact support contained in $\mathbb{R}^N$. The velocity field

$$V(s)(x) = V(s,x), \qquad x \in D, \quad s \geq 0$$

belongs to $\mathscr{D}^k(\bar{D},\mathbb{R}^N)$ for each s. It can generate transformations

$$T_s(V)X = x(s,X), \quad s \geq 0, \quad X \in D$$

through the following dynamical system

$$\begin{cases} \frac{\mathrm{d}x}{\mathrm{d}s}(s,X) = V(s,x(s)) \\ x(0,X) = X \end{cases} \tag{1}$$

with the initial value X given. We denote the "transformed domain" $T_s(V)(\Omega)$ by $\Omega_s(V)$ at $s \geq 0$, and also set $\partial\Omega_s := T_s(\partial\Omega)$.

There exists an interval $I = [0,\delta)$, $0 < \delta \leq \varepsilon$, and a one-to-one map T_s from $\bar{D}$ onto $\bar{D}$ such that

(i) $T_0 = \mathrm{I}$;

(ii) $(s,x) \mapsto T_s(x)$ belongs to $C^1(I;C^k(D;D))$ with $T_s(\partial D) = \partial D$;

(iii) $(s,x) \mapsto T_s^{-1}(x)$ belongs to $C(I;C^k(D;D))$.

Such transformation are well studied in Delfour and Zolesio (2002).

Furthermore, for sufficiently small $s > 0$, the Jacobian J_s is strictly positive:

$$J_s(x) := |\det(\mathrm{D}T_s(x))| = \det \mathrm{D}T_s(x) > 0,\ (\mathrm{D}T_s)_{ij} = \partial_j (T_s)_i \tag{2}$$

where $\mathrm{D}T_s(x)$ denotes the Jacobian matrix of the transformation T_s evaluated at a point $x \in D$ associated with the velocity field V. We will also use the following notation: $\mathrm{D}T_s^{-1}(x)$ is the inverse of the matrix $\mathrm{D}T_s(x)$, ${}^*\mathrm{D}T_s^{-1}(x)$ is the transpose of the matrix $\mathrm{D}T_s^{-1}(x)$. These quantities also satisfy the following lemmas.

Lemma 2.1 (Sokolowski and Zolesio (1992)) *For any $V \in E^k$, $\mathrm{D}T_s$ and J_s are invertible. Moreover, $\mathrm{D}T_s$, $\mathrm{D}T_s^{-1}$ are in $C^1([0,\varepsilon];C^{k-1}(\bar{D};\mathbb{R}^{N\times N}))$, and J_s, J_s^{-1} are in $C^1([0,\varepsilon];C^{k-1}(\bar{D};\mathbb{R}))$*

Lemma 2.2 (Sokolowski and Zolesio (1992)) *φ is assumed to be a vector function in $C^1(D)^N$.*

(1) $\mathrm{D}(T_s^{-1}) \circ T_s = \mathrm{D}T_s^{-1}$;

(2) $\mathrm{D}(\varphi \circ T_s^{-1}) = (\mathrm{D}\varphi \cdot \mathrm{D}T_s^{-1}) \circ T_s^{-1}$;

(3) $(\mathrm{D}\varphi) \circ T_s = \mathrm{D}(\varphi \circ T_s) \cdot \mathrm{D}T_s^{-1}$.

Now let $J(\Omega)$ be a real valued functional associated with any regular domain Ω, we say that this functional has a **Eulerian derivative** at Ω in the direction V if the limit

$$\lim_{s \searrow 0} \frac{J(\Omega_s) - J(\Omega)}{s} := \mathrm{d}J(\Omega;V)$$

exists.

Furthermore, if the map

$$V \mapsto \mathrm{d}J(\Omega;V):\ \mathrm{E}^k \to \mathbb{R}$$

is linear and continuous, we say that J is **shape differentiable** at Ω. In the distributional sense we have

$$\mathrm{d}J(\Omega;V) = \langle \nabla J, V \rangle_{\mathscr{D}^k(\bar{D},\mathbb{R}^N)' \times \mathscr{D}^k(\bar{D},\mathbb{R}^N)}. \tag{3}$$

When J has a Eulerian derivative, we say that ∇J is the **shape gradient** of J at Ω.

Given $T > 0$, we introduce the notation $L^p(0,T;X)$ which denotes the space of L^p integrable functions f from $[0,T]$ into the Banach space X with the norm

$$\|f\|_{L^p(0,T;X)} = \left(\int_0^T \|f\|_X^p \,\mathrm{d}t \right)^{1/p}, \quad 1 \leq p < +\infty.$$

We also denote by $L^\infty(0,T;X)$ the space of essentially bounded functions f from $[0,T]$ into X, and is equipped with the Banach norm

$$\operatorname*{ess\,sup}_{t\in[0,T]} \|f(t)\|_X.$$

Before closing this subsection, we introduce the following functional spaces which will be used in this paper:

$$\begin{aligned}
V^k(\Omega) &:= \{u \in H^k(\Omega)^N :\ u = 0 \text{ on } \Gamma_w \cup \Gamma_0\},\\
V_g^k(\Omega) &:= \{u \in H^k(\Omega)^N :\ u = 0 \text{ on } \Gamma_w \cup \Gamma_0,\ u = g_1 \text{ on } \Gamma_u\},\\
V_0^k(\Omega) &:= \{u \in H^k(\Omega)^N :\ u = 0 \text{ on } \Gamma_w \cup \Gamma_u \cup \Gamma_0\},\\
Q^k(\Omega) &:= \left\{ p \in H^k(\Omega) : \int_\Omega p \,\mathrm{d}x = 0 \text{ (if } \mathrm{meas}(\Gamma_d) = 0) \right\}.
\end{aligned}$$

2.2 Formulation of the flow optimization problem

Consider a flow region $\Omega \in \mathbb{R}^2$, with its boundary Γ, that is occupied by a fluid of kinematic viscosity ν. The governing equations for a viscous incompressible flow in Ω are given as

$$\partial_t y - \operatorname{div} \sigma(y,p) + \mathrm{D}y \cdot y = 0 \qquad \text{in } \Omega \times (0,T), \tag{4}$$

$$\operatorname{div} y = 0 \qquad \text{in } \Omega \times (0,T), \tag{5}$$

where y denotes the velocity field, p the pressure, and $\sigma(y,p)$ the stress tensor defined by $\sigma(y,p) := -p\mathrm{I} + 2\nu\varepsilon(y)$ with the rate of deformation tensor $\varepsilon(y) := (\mathrm{D}y + {}^*\mathrm{D}y)/2$, where ${}^*\mathrm{D}y$ denotes the transpose of the matrix $\mathrm{D}y$ and I denotes the identity tensor. $(0,T)$ is the time interval during which the flow is considered.

(4) and (5) have to be completed by further conditions, such as the following initial condition which consists of a specified divergence-free velocity field:

$$y(0) = y_0 \quad \text{in } \Omega \tag{6}$$

and boundary conditions. Let us consider the isolated body problem described in Figure 1, corresponding to an external flow around a solid body S.

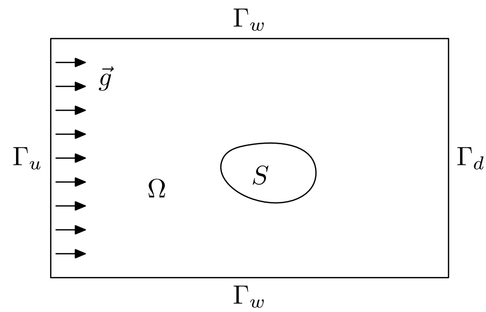

Figure 1: External flow around a solid body S.

We reduce the problem to a bounded domain D by introducing an artificial boundary ∂D which has to be taken sufficiently far from S so that the corresponding flow is a good approximation of the unbounded external flow around S and $\Omega := D \backslash \bar{S}$ is the effective domain. Typical boundary conditions are

$$y = g_1 \qquad \text{on } \Gamma_u \times (0,T) \tag{7}$$

$$y = 0 \qquad \text{on } (\Gamma_0 \cup \Gamma_w) \times (0,T) \tag{8}$$

$$\sigma(y,p) \cdot n = g_2 \qquad \text{on } \Gamma_d \times (0,T), \tag{9}$$

where n denotes the unit vector of outward normal on $\Gamma = \Gamma_u \cup \Gamma_d \cup \Gamma_w \cup \Gamma_0$, Γ_u is the inflow boundary, Γ_d the outflow boundary, Γ_w the boundary corresponding to the fluid wall and Γ_0 is the boundary which is to be optimized. We also recall that the Reynolds number Re is classically defined by $\mathrm{Re} = UL/\nu$ with U a characteristic velocity and L a characteristic length.

Our goal is to find a shape Ω such that a given cost functional J which depends on $y(x,t)$, $p(x,t)$ and on Ω itself, is minimized. The optimal shape design problem is given as follows.

$$\begin{cases} \text{minimize } J(\Omega) \text{ subject to } (4)-(9) \\ \text{with } \Omega \in \mathscr{O} := \left\{\Omega \subset \mathbb{R}^N : \ \Gamma_u \cup \Gamma_d \cup \Gamma_w \text{ is fixed}, \ \int_\Omega \mathrm{d}x = \text{constant}\right\}. \end{cases} \tag{10}$$

We consider

$$J(\Omega) = \int_{t_L}^{t_U} \Phi(y)\,\mathrm{d}t = 2\nu \int_{t_L}^{t_U} \int_\Omega |\varepsilon(y)|^2\,\mathrm{d}x\,\mathrm{d}t, \tag{11}$$

where $[t_L, t_U]$ is a characteristic time interval and $\Phi(y)$ is the viscous dissipation energy which is due to the work done by the pressure and frictional shear forces acting on the boundary of the flow region. Definitions of t_L and t_U are problem dependent. For instance, if the optimization problem involves flow with initial condition generated transients that are damped out, the interval starts at the initial time and ends after the steady state is reached.

3 Function space parametrization

In this section we derive the structure of the continuous shape gradient for the cost functional $J(\Omega)$ by function space parametrization techniques in order to bypass the usual study of material derivative.

Let Ω be of class C^2, the weak formulation of (4)–(6) in mixed form is:

$$\begin{cases} \forall t \in (0,T),\ \text{seek}\ (y(t),p(t)) \in V_g^2(\Omega) \times Q^1(\Omega)\ \text{such that} \\ \int_\Omega [\partial_t y \cdot v + 2\nu\varepsilon(y) : \varepsilon(v) + \mathrm{D}y \cdot y \cdot v - p \,\mathrm{div}\, v]\,\mathrm{d}x \\ \qquad\qquad = \int_{\Gamma_d} g_2 \cdot v \,\mathrm{d}s,\ \forall v \in V_0^2(\Omega), \\ \int_\Omega \mathrm{div}\, y q \,\mathrm{d}x = 0,\ \forall q \in Q^1(\Omega), \\ y(0) = y_0. \end{cases} \tag{12}$$

Where in the weak form (12), we have used the following lemma.

Lemma 3.1

$$2\int_\Omega \varepsilon(y) : \varepsilon(v)\,\mathrm{d}x = -\int_\Omega (\Delta y + \nabla \,\mathrm{div}\, y) \cdot v \,\mathrm{d}x + 2\int_{\partial\Omega} \varepsilon(y) \cdot n \cdot v \,\mathrm{d}s.$$

Now we introduce the following Lagrange functional associated with (12) and (11):

$$G(\Omega, y, p, v, q) = J(\Omega) - L(\Omega, y, p, v, q), \tag{13}$$

where

$$L(\Omega, y, p, v, q) = \int_0^T \int_\Omega [-\partial_t v \cdot y + 2\nu\varepsilon(y) : \varepsilon(v) + \mathrm{D}y \cdot y \cdot v - p \,\mathrm{div}\, v \\ - \mathrm{div}\, y q]\,\mathrm{d}x\,\mathrm{d}t - \int_0^T \int_{\Gamma_d} g_2 \cdot v \,\mathrm{d}s\,\mathrm{d}t + \int_\Omega y(T) \cdot v(T)\,\mathrm{d}x - \int_\Omega y_0 \cdot v(0)\,\mathrm{d}x.$$

The minimization problem (10) can be put in the following form

$$\min_{\Omega \in \mathscr{O}} \ \min_{(y,p) \in \mathscr{V}_g^2(\Omega) \times \mathscr{Q}^1(\Omega)} \ \max_{(v,q) \in \mathscr{V}_0^2(\Omega) \times \mathscr{Q}^1(\Omega)} G(\Omega, y, p, v, q), \tag{14}$$

where

$$\mathscr{V}_g^2(\Omega) := L^2(0,T; V_g^2(\Omega)), \quad \mathscr{V}_0^2(\Omega) := L^2(0,T; V_0^2(\Omega)),$$

$\mathscr{Q}^1(\Omega) := L^2(0,T;Q^1(\Omega))$.

We can use the minimax framework to avoid the study of the state derivative. The Karusch-Kuhn-Tucker conditions will furnish the shape gradient of the cost functional $J(\Omega)$ by using the adjoint system. Now let's establish the first optimality condition for the problem

$$\min_{(y,p)\in\mathscr{V}_g^2(\Omega)\times\mathscr{Q}^1(\Omega)} \max_{(v,q)\in\mathscr{V}_0^2(\Omega)\times\mathscr{Q}^1(\Omega)} G(\Omega,y,p,v,q). \tag{15}$$

Formally the adjoint equations are defined from the Euler–Lagrange equations of the Lagrange functional G. Clearly, the variation of G with respect to (v,q) can recover the state system (12). On the other hand, in order to find the adjoint state system, we differentiate G with respect to p in the direction δp,

$$\frac{\partial G}{\partial p}(\Omega,y,p,v,q)\cdot\delta p = \int_0^T\int_\Omega \delta p\,\mathrm{div}\,v\,\mathrm{d}x\,\mathrm{d}t = 0,$$

Taking δp with compact support in Ω gives

$$\mathrm{div}\,v = 0. \tag{16}$$

Then we differentiate G with respect to y in the direction δy and employ Green formula,

$$\begin{aligned}
&\frac{\partial G}{\partial y}(\Omega,y,p,v,q)\cdot\delta y = \\
&\int_0^T\int_\Omega(-2\chi(t)\nu\Delta y+\partial_t v+\nu\Delta v-\nabla q-{}^*\mathrm{D}y\cdot v+\mathrm{D}v\cdot y)\cdot\delta y\,\mathrm{d}x\,\mathrm{d}t\\
&-\int_0^T\int_{\partial\Omega}\sigma(v,q)\cdot n\cdot\delta y\,\mathrm{d}s\,\mathrm{d}t+4\int_0^T\int_{\partial\Omega}\chi(t)\nu\varepsilon(y)\cdot n\cdot\delta y\,\mathrm{d}s\,\mathrm{d}t\\
&\qquad\qquad-\int_0^T\int_{\partial\Omega}(y\cdot n)(v\cdot\delta y)\,\mathrm{d}s\,\mathrm{d}t+\int_\Omega\delta y(T)\cdot v(T)\,\mathrm{d}x,
\end{aligned}$$

where

$$\chi(t)=\begin{cases}0 & o\le t<t_L,\\ 1 & t_L\le t\le t_U.\end{cases}$$

Taking δy with compact support in Ω gives

$$\partial_t v+\nu\Delta v-\nabla q-{}^*\mathrm{D}y\cdot v+\mathrm{D}v\cdot y = 2\chi(t)\nu\Delta y. \tag{17}$$

Then varying δy on Γ_d gives

$$\sigma(v,q)\cdot n + (y\cdot n)v - 4\chi(t)\nu\varepsilon(y)\cdot n = 0, \qquad \text{on } \Gamma_d \times (0,T). \tag{18}$$

Finally we obtain the following adjoint state system

$$\begin{cases} -\partial_t v - \operatorname{div}\sigma(v,q) + {}^*\mathrm{D}y\cdot v - \mathrm{D}v\cdot y = -2\chi(t)\nu\Delta y & \text{in } \Omega\times(0,T) \\ \operatorname{div} v = 0 & \text{in } \Omega\times(0,T) \\ \sigma(v,q)\cdot n + (y\cdot n)v - 4\chi(t)\nu\varepsilon(y)\cdot n = 0, & \text{on } \Gamma_d\times(0,T) \\ v = 0 & \text{on } (\Gamma_u\cup\Gamma_w\cup\Gamma_0)\times(0,T) \\ v(T) = 0 & \text{in } \Omega, \end{cases} \tag{19}$$

and its variational form

$$\begin{cases} \forall t\in(0,T),\ \text{seek } (v,q)\in V_0^2(\Omega)\times Q^1(\Omega) \text{ such that} \\ \int_\Omega[-\partial_t v\cdot\varphi + 2\nu\varepsilon(v):\varepsilon(\varphi) + \mathrm{D}\varphi\cdot y\cdot v + \mathrm{D}y\cdot\varphi\cdot v - q\operatorname{div}\varphi]\,\mathrm{d}x \\ \qquad\qquad = 4\nu\chi(t)\int_\Omega \varepsilon(y):\varepsilon(\varphi)\,\mathrm{d}x, \quad \forall\varphi\in V_0^2(\Omega), \\ \int_\Omega \operatorname{div} v\,\psi\,\mathrm{d}x = 0, \quad \forall\psi\in Q^1(\Omega), \\ v(T) = 0. \end{cases} \tag{20}$$

We employ the velocity method to modelize the domain deformations. We only perturb the boundary Γ_0 and consider the mapping $T_s(V)$, the flow of the velocity field

$$V\in V_{\mathrm{ad}} := \{V\in C^0(0,\tau;C^2(\mathbb{R}^N)^N) : V = 0 \text{ in the neighorhood of } \Gamma_u\cup\Gamma_w\cup\Gamma_d\}.$$

Our objective in this section is to study the derivative of $j(s)$ with respect to s, where

$$j(s) := \min_{(y_s,p_s)\in\mathscr{V}_g^2(\Omega_s)\times\mathscr{Q}^1(\Omega_s)} \ \max_{(v_s,q_s)\in\mathscr{V}_0^2(\Omega_s)\times\mathscr{Q}^1(\Omega_s)} G(\Omega_s,y_s,p_s,v_s,q_s), \tag{21}$$

(y_s,p_s) and (v_s,q_s) satisfy (12) and (20) on the perturbed domain Ω_s, respectively. Unfortunately, the Sobolev space $V_g^2(\Omega_s)$, $V_0^2(\Omega_s)$, and $Q^1(\Omega_s)$ depend on the parameter s, so we need to introduce the so-called function space parametrization technique which consists in transporting the different quantities (such as, a cost functional) defined on the variable domain Ω_s back into the reference domain Ω

which does not depend on the perturbation parameter s. Thus we can use differential calculus since the functionals involved are defined in a fixed domain Ω with respect to the parameter s.

To do this, we define the following parametrizations

$$
\begin{aligned}
V_g^2(\Omega_s) &= \{y \circ T_s^{-1} : y \in V_g^2(\Omega)\}; \\
V_0^2(\Omega_s) &= \{v \circ T_s^{-1} : v \in V_0^2(\Omega)\}; \\
Q^1(\Omega_s) &= \{p \circ T_s^{-1} : p \in Q^1(\Omega)\}.
\end{aligned}
$$

where "$\circ$" denotes the composition of the two maps.

Note that since T_s and T_s^{-1} are diffeomorphisms, these parametrizations can not change the value of the saddle point. We can rewrite (21) as

$$
j(s) = \min_{(y,p)\in\mathscr{V}_g^2(\Omega)\times\mathscr{Q}^1(\Omega)} \max_{(v,q)\in\mathscr{V}_0^2(\Omega)\times\mathscr{Q}^1(\Omega)} G(\Omega_s, y\circ T_s^{-1}, p\circ T_s^{-1}, v\circ T_s^{-1}, q\circ T_s^{-1}). \tag{22}
$$

where the Lagrangian

$$
G(\Omega_s, y\circ T_s^{-1}, p\circ T_s^{-1}, v\circ T_s^{-1}, q\circ T_s^{-1}) = I_1(s) + I_2(s) + I_3(s)
$$

with

$$
I_1(s) := 2\nu \int_0^T \int_{\Omega_s} \chi(t) |\varepsilon(y\circ T_s^{-1})|^2 \,\mathrm{d}x\,\mathrm{d}t,
$$

$$
\begin{aligned}
I_2(s) := -\int_0^T \int_{\Omega_s} &[-\partial_t (v\circ T_s^{-1}) \cdot (y\circ T_s^{-1}) + 2\nu\varepsilon(v\circ T_s^{-1}) : \varepsilon(y\circ T_s^{-1}) \\
&+ \mathrm{D}(y\circ T_s^{-1}) \cdot (y\circ T_s^{-1}) \cdot (v\circ T_s^{-1}) - (p\circ T_s^{-1})\,\mathrm{div}\,(v\circ T_s^{-1}) \\
&- \mathrm{div}\,(y\circ T_s^{-1})(q\circ T_s^{-1})] \,\mathrm{d}x\,\mathrm{d}t,
\end{aligned}
$$

and

$$
I_3(s) := \int_0^T \int_{\Gamma_d} g_2 \cdot v \,\mathrm{d}s\,\mathrm{d}t - \int_{\Omega_s} [(y(T)\circ T_s^{-1}) \cdot (v(T)\circ T_s^{-1}) - y_0 \cdot (v(0)\circ T_s^{-1})] \,\mathrm{d}x.
$$

Now we introduce the theorem concerning on the differentiability of a saddle point (or a minimax). To begin with, some notations are given as follows.

Define a functional

$$
\mathscr{G} : [0,\tau] \times X \times Y \to \mathbb{R}
$$

with $\tau > 0$, and X, Y are the two topological spaces.

For any $t \in [0, \tau]$, define $g(t) = \inf_{x\in X} \sup_{y\in Y} \mathscr{G}(t,x,y)$ and the sets

$$X(t) = \{x^t \in X : g(t) = \sup_{y\in Y} \mathscr{G}(t,x^t,y)\}$$
$$Y(t,x) = \{y^t \in Y : \mathscr{G}(t,x,y^t) = \sup_{y\in Y} \mathscr{G}(t,x,y)\}$$

Similarly, we can define the dual functional $h(t) = \sup_{y\in Y} \inf_{x\in X} \mathscr{G}(t,x,y)$ and the corresponding sets

$$Y(t) = \{y^t \in Y : h(t) = \inf_{x\in X} \mathscr{G}(t,x,y^t)\}$$
$$X(t,y) = \{x^t \in X : \mathscr{G}(t,x^t,y) = \inf_{x\in X} \mathscr{G}(t,x,y)\}$$

Furthermore, we introduce the set of saddle points

$$S(t) = \{(x,y) \in X \times Y : g(t) = \mathscr{G}(t,x,y) = h(t)\}$$

Now we can introduce the following theorem (see Correa and Seeger (1985) or page 427 of Delfour and Zolesio (2002)):

Theorem 3.1 *Assume that the following hypothesis hold:*

(H1) $S(t) \neq \emptyset$, $t \in [0, \tau]$;

(H2) The partial derivative $\partial_t \mathscr{G}(t,x,y)$ *exists in* $[0,\tau]$ *for all*

$$(x,y) \in \left[\bigcup_{t\in[0,\tau]} X(t) \times Y(0)\right] \bigcup \left[X(0) \times \bigcup_{t\in[0,\tau]} Y(t)\right];$$

(H3) There exists a topology $\mathscr{T}_X$ *on* X *such that for any sequence* $\{t_n : t_n \in [0,\tau]\}$ *with* $\lim_{n\nearrow\infty} t_n = 0$, *there exists* $x^0 \in X(0)$ *and a subsequence* $\{t_{n_k}\}$, *and for each* $k \geq 1$, *there exists* $x_{n_k} \in X(t_{n_k})$ *such that*

  (i) $\lim_{n\nearrow\infty} x_{n_k} = x^0$ *in the* $\mathscr{T}_X$ *topology,*

  (ii) $\liminf_{\substack{t\searrow 0\\ k\nearrow\infty}} \partial_t \mathscr{G}(t,x_{n_k},y) \geq \partial_t \mathscr{G}(0,x^0,y), \quad \forall y \in Y(0);$

(H4) There exists a topology $\mathscr{T}_Y$ *on* Y *such that for any sequence* $\{t_n : t_n \in [0,\tau]\}$ *with* $\lim_{n\nearrow\infty} t_n = 0$, *there exists* $y^0 \in Y(0)$ *and a subsequence* $\{t_{n_k}\}$, *and for each* $k \geq 1$, *there exists* $y_{n_k} \in Y(t_{n_k})$ *such that*

  (i) $\lim_{n\nearrow\infty} y_{n_k} = y^0$ *in the* $\mathscr{T}_Y$ *topology,*

(ii) $\limsup_{\substack{t\searrow 0\\ k\nearrow\infty}} \partial_t \mathscr{G}(t,x,y_{n_k}) \le \partial_t \mathscr{G}(0,x,y^0), \quad \forall x \in X(0).$

Then there exists $(x^0,y^0) \in X(0)\times Y(0)$ *such that*

$$\begin{aligned}\mathrm{d}g(0) &= \lim_{t\searrow 0} \frac{g(t)-g(0)}{t} \\ &= \inf_{x\in X(0)} \sup_{y\in Y(0)} \partial_t \mathscr{G}(0,x,y) = \partial_t \mathscr{G}(0,x^0,y^0) = \sup_{y\in Y(0)} \inf_{x\in X(0)} \partial_t \mathscr{G}(0,x,y) \end{aligned} \tag{23}$$

This means that $(x^0,y^0) \in X(0)\times Y(0)$ *is a saddle point of* $\partial_t \mathscr{G}(0,x,y)$.

Following Theorem 3.1, we need to differentiate the perturbed Lagrange functional $G(\Omega_s, y\circ T_s^{-1}, p\circ T_s^{-1}, v\circ T_s^{-1}, q\circ T_s^{-1})$.
To perform the differentiation, we introduce the following Hadamard formula (see Hadamard (1907))

$$\frac{\mathrm{d}}{\mathrm{d}s}\int_{\Omega_s} F(s,x)\,\mathrm{d}x = \int_{\Omega_s} \frac{\partial F}{\partial s}(s,x)\,\mathrm{d}x + \int_{\partial\Omega_s} F(s,x)\,V\cdot n_s\,\mathrm{d}s, \tag{24}$$

for a sufficiently smooth functional $F : [0,\tau]\times\mathbb{R}^N \to \mathbb{R}$.
By Hadamard formula (24), we get

$$\partial_t G(\Omega_s, y\circ T_s^{-1}, p\circ T_s^{-1}, v\circ T_s^{-1}, q\circ T_s^{-1}) = I_1'(0) + I_2'(0) + I_3'(0),$$

where

$$I_1'(0) = 4\nu \int_0^T \int_\Omega \chi(t)\varepsilon(y) : \varepsilon(-\mathrm{D}y\cdot V)\,\mathrm{d}x\,\mathrm{d}t + 2\nu \int_0^T \int_{\Gamma_0} \chi(t)|\varepsilon(y)|^2 V_n\,\mathrm{d}s\,\mathrm{d}t; \tag{25}$$

$$\begin{aligned} I_2'(0) &= \int_0^T \int_\Omega [\partial_t(-\mathrm{D}v\cdot V)\cdot y + \partial_t v\cdot(-\mathrm{D}y\cdot V)]\,\mathrm{d}x\,\mathrm{d}t \\ &- \int_0^T \int_\Omega [2\nu\varepsilon(-\mathrm{D}y\cdot V)\cdot\varepsilon(v) + 2\nu\varepsilon(y)\cdot\varepsilon(-\mathrm{D}v\cdot V) + \mathrm{D}y\cdot y\cdot(-\mathrm{D}y\cdot V) \\ &+ \mathrm{D}(-\mathrm{D}y\cdot V)\cdot y\cdot v + \mathrm{D}y\cdot(-\mathrm{D}y\cdot V)\cdot v - p\,\mathrm{div}\,(-\mathrm{D}v\cdot V) \\ &- \mathrm{div}\,(-\mathrm{D}y\cdot V)q - \mathrm{div}\,y(-\nabla q\cdot V) - (-\nabla p\cdot V)\,\mathrm{div}\,v]\,\mathrm{d}x\,\mathrm{d}t \\ &\quad + \int_0^T \int_{\Gamma_0} (\partial_t v\cdot y - 2\nu\varepsilon(y):\varepsilon(v) - \mathrm{D}y\cdot y\cdot v + p\,\mathrm{div}\,v + \mathrm{div}\,yq)V_n\,\mathrm{d}s\,\mathrm{d}t; \end{aligned} \tag{26}$$

and

$$I_3'(0) = -\int_\Omega [(-\mathrm{D}y(T)\cdot V)\cdot v(T) + y(T)\cdot(-\mathrm{D}v(T)\cdot V)]\,\mathrm{d}x - \int_{\Gamma_0} y(T)\cdot v(T)V_n\,\mathrm{d}s$$
$$+ \int_\Omega y_0\cdot(-\mathrm{D}v(0)\cdot V)\,\mathrm{d}x + \int_{\Gamma_0} y_0\cdot v(0)V_n\,\mathrm{d}s. \quad (27)$$

To simplify (25) and (26), we introduce the following lemma.

Lemma 3.2 *If two vector functions y and v vanish on the boundary Γ_0 and $\operatorname{div} y = \operatorname{div} v = 0$ in Ω, the following identities*

$$\mathrm{D}y\cdot V\cdot n = (\mathrm{D}y\cdot n\cdot n)V_n = \operatorname{div} y V_n; \quad (28)$$
$$\varepsilon(y):\varepsilon(v) = \varepsilon(y):(\varepsilon(v)\cdot(n\otimes n)) = (\varepsilon(y)\cdot n)\cdot(\varepsilon(v)\cdot n); \quad (29)$$
$$(\varepsilon(y)\cdot n)\cdot(\mathrm{D}v\cdot V) = (\varepsilon(y)\cdot n)\cdot(\mathrm{D}v\cdot n)V_n = (\varepsilon(y)\cdot n)\cdot(\varepsilon(v)\cdot n)V_n \quad (30)$$

hold on the boundary Γ_0, where the tensor product $n\otimes n := \sum_{i,j=1}^N n_i n_j$.

Using Lemma 3.1, for (25) we have

$$I_1'(0) = -2\nu\int_0^T\int_\Omega \chi(t)\Delta y\cdot(-\mathrm{D}y\cdot V)\,\mathrm{d}x\,\mathrm{d}t$$
$$+4\nu\int_0^T\int_{\Gamma_0}\chi(t)(\varepsilon(y)\cdot n)\cdot(-\mathrm{D}y\cdot V)\,\mathrm{d}s\,\mathrm{d}t + 2\nu\int_0^T\int_{\Gamma_0}\chi(t)|\varepsilon(y)|^2 V_n\,\mathrm{d}s\,\mathrm{d}t.$$

By the identities (29) and (30), we further get

$$I_1'(0) = -2\nu\int_0^T\int_\Omega \chi(t)\Delta y\cdot(-\mathrm{D}y\cdot V)\,\mathrm{d}x\,\mathrm{d}t - 2\nu\int_0^T\int_{\Gamma_0}\chi(t)|\varepsilon(y)|^2 V_n\,\mathrm{d}s\,\mathrm{d}t. \quad (31)$$

Employing Lemma 3.1 and $y|_{\Gamma_0} = V|_{\Gamma_w\cup\Gamma_u\cup\Gamma_d} = 0$, (26) can be rewritten as

$$I_2'(0) = \int_0^T\int_\Omega [(-\partial_t y + \nu\Delta y - \mathrm{D}y\cdot y - \nabla p)\cdot(-\mathrm{D}v\cdot V) + \operatorname{div} y(-\nabla q\cdot V)]\,\mathrm{d}x\,\mathrm{d}t$$
$$+\int_0^T\int_\Omega [(\partial_t v + \nu\Delta v + \mathrm{D}v\cdot y - {}^*\mathrm{D}y\cdot v - \nabla q)\cdot(-\mathrm{D}y\cdot V) + \operatorname{div} v(-\nabla p\cdot V)]\,\mathrm{d}x\,\mathrm{d}t$$
$$-\int_0^T\int_{\Gamma_0}[\sigma(y,p)\cdot n\cdot(-\mathrm{D}v\cdot V) + \sigma(v,q)\cdot n\cdot(-\mathrm{D}y\cdot V)]\,\mathrm{d}s\,\mathrm{d}t$$
$$+\int_0^T\int_{\Gamma_0}[\partial_t v\cdot y - 2\nu\varepsilon(y):\varepsilon(v) - \mathrm{D}y\cdot y\cdot v + p\operatorname{div} v + \operatorname{div} y q]V_n\,\mathrm{d}s\,\mathrm{d}t$$
$$+\int_\Omega [(-\mathrm{D}v\cdot V)(T)\cdot y(T) - (-\mathrm{D}v\cdot V)(0)\cdot y(0)]\,\mathrm{d}x. \quad (32)$$

Since (y,p) and (v,q) satisfy (4)–(6) and (19) respectively, (32) reduces to

$$\begin{aligned}I_2'(0) &= 2\nu \int_0^T \int_\Omega \chi(t)\Delta y\cdot(-\mathrm{D}y\cdot V)\,\mathrm{d}x\,\mathrm{d}t \\ &- \int_0^T \int_{\Gamma_0} [\sigma(y,p)\cdot n\cdot(-\mathrm{D}v\cdot V) + \sigma(v,q)\cdot n\cdot(-\mathrm{D}y\cdot V) + 2\nu\varepsilon(y):\varepsilon(v)V_n]\,\mathrm{d}s\,\mathrm{d}t \\ &+ \int_\Omega [(-\mathrm{D}v\cdot V)(T)\cdot y(T) - (-\mathrm{D}v\cdot V)(0)\cdot y(0)]\,\mathrm{d}x. \end{aligned} \tag{33}$$

On the boundary Γ_0, we can deduce that

$$\begin{aligned} &-\sigma(y,p)\cdot n\cdot(-\mathrm{D}v\cdot V) - \sigma(v,q)\cdot n\cdot(-\mathrm{D}y\cdot V) \\ &= 2\nu[\varepsilon(y)\cdot n\cdot(\mathrm{D}v\cdot V) + \varepsilon(v)\cdot n\cdot(\mathrm{D}y\cdot V)] && \text{(by (28))} \\ &= 4\nu(\varepsilon(y)\cdot n)\cdot(\varepsilon(v)\cdot n)V_n && \text{(by (30))} \\ &= 4\nu\varepsilon(y):\varepsilon(v)V_n. && \text{(by (29))} \end{aligned}$$

Therefore, (33) becomes

$$\begin{aligned}I_2'(0) &= 2\nu \int_0^T \int_\Omega \chi(t)\Delta y\cdot(-\mathrm{D}y\cdot V)\,\mathrm{d}x\,\mathrm{d}t + 2\nu \int_0^T \int_{\Gamma_0} \varepsilon(y):\varepsilon(v)V_n\,\mathrm{d}s\,\mathrm{d}t \\ &+ \int_\Omega [(-\mathrm{D}v\cdot V)(T)\cdot y(T) - (-\mathrm{D}v\cdot V)(0)\cdot y(0)]\,\mathrm{d}x. \end{aligned} \tag{34}$$

Adding (31), (34) and (27) together, and then using $v|_{\Gamma_0} = 0$ and $v(T) = 0$ in Ω, we finally obtain the boundary expression for the Eulerian derivative of $J(\Omega)$,

$$\mathrm{d}J(\Omega;V) = 2\nu \int_0^T \int_{\Gamma_0} \left[\varepsilon(y):\varepsilon(v) - \chi(t)|\varepsilon(y)|^2\right] V_n\,\mathrm{d}s\,\mathrm{d}t, \tag{35}$$

Finally for each $t \in [0,T]$, since the mapping $V \mapsto \mathrm{d}J(\Omega;V)$ is linear and continuous, we get the expression for the shape gradient

$$\nabla J = 2\nu[\varepsilon(y):\varepsilon(v) - \chi(t)|\varepsilon(y)|^2]n \tag{36}$$

by (3).

4 Time and space approximation of our problem

In general it is impossible to solve the infinite dimensional shape optimization problem, so we resort to numerical approximation in both space and time.

4.1 Semidiscrete-in-time approximation

To discretize the state system (12) in time, we use a semi-implicit Oseen–Crank–Nicolson scheme. Let $0 = t_0 < \cdots < t_L < \cdots < t_U = T$ be a uniform partition in the time dimension. We will denote by q the vector $(q^0, q^1, \cdots, q^L, \cdots, q^U)$ defined discretely with respect to time.

The state variables $\mathbf{y} = (y^0, y^1, \cdots, y^U) \in V^1(\Omega)$ and $\mathrm{p} = (p^0, p^1, \cdots, p^U) \in Q^0(\Omega)$ are constrained to satisfy the following semidiscrete system

$$\begin{cases} \int_\Omega \left[\frac{1}{\Delta t}(y^n - y^{n-1})\cdot v + 2\nu\varepsilon(y^{n-\frac{1}{2}}) : \varepsilon(v) + \mathrm{D}y^{n-\frac{1}{2}}\cdot y^{n-1}\cdot v - p^{n-\frac{1}{2}}\operatorname{div} v\right]\mathrm{d}x \\ \qquad\qquad = \int_{\Gamma_d} g_2^{n-\frac{1}{2}}\cdot v\,\mathrm{d}s,\ \forall v \in V_0^1(\Omega),\ \text{for } n = 1,\cdots,U, \\ \int_\Omega \operatorname{div} y^{n-\frac{1}{2}} q\,\mathrm{d}x = 0,\ \forall q \in Q^0(\Omega),\ \text{for } n = 1,\cdots,U, \\ y^{n-\frac{1}{2}}|_{\Gamma_u} = g_1^{n-\frac{1}{2}},\ \text{for } n = 1,\cdots,U, \\ y^0 = y_0, \quad \text{in } \Omega. \end{cases} \tag{37}$$

Where the notations

$$\Delta t = t_n - t_{n-1},\ y^{n-\frac{1}{2}} = \frac{1}{2}(y^{n-1} + y^n),\ p^{n-\frac{1}{2}} = \frac{1}{2}(p^{n-1} + p^n),\ g_i^{n-\frac{1}{2}} = \frac{1}{2}(g_i^{n-1} + g_i^n),$$

with y^n, p^n, g_1^n and g_2^n are approximated values of y, p, g_1 and g_2 at time t_n, respectively.

At each time in (37), we only need to solve a linear problem, a steady Oseen problem, since the nonlinear term is treated linear. This scheme is second order accurate in time (see Quarteroni and Valli (1994)).

The adjoint variables $\mathbf{v} = (v^0, v^1, \cdots, v^U) \in V_0^1(\Omega)$ and $\mathrm{q} = (q^0, q^1, \cdots, q^U) \in Q^0(\Omega)$ are constrained to satisfy the following semidiscrete system

$$\begin{cases} \int_\Omega [-\frac{1}{\Delta t}(v^n - v^{n-1})\cdot\varphi + 2\nu\varepsilon(v^{n-\frac{1}{2}}) : \varepsilon(\varphi) + \mathrm{D}\varphi\cdot y^n\cdot v^{n-\frac{1}{2}} \\ \quad + \mathrm{D}y^n\cdot\varphi\cdot v^{n-\frac{1}{2}} - q^{n-\frac{1}{2}}\operatorname{div}\varphi]\,\mathrm{d}x = 4\nu\chi(n\Delta t)\int_\Omega \varepsilon(y^n) : \varepsilon(\varphi)\,\mathrm{d}x,\ \forall\varphi \in V_0^1(\Omega), \\ \int_\Omega \operatorname{div} v^{n-\frac{1}{2}}\psi\,\mathrm{d}x = 0, \quad \forall\psi \in Q^0(\Omega),\ \text{for } n = 1,\cdots,U. \\ v^U = 0, \qquad \text{in } \Omega. \end{cases} \tag{38}$$

4.2 Full discrete time–space approximation

We make the additional assumption that Ω is a bounded polygonal domain of $\mathbb{R}^2$ and only consider the conforming finite element approximations. Let $X_h \subset H^1(\Omega)^N$

and $S_h \subset L^2(\Omega)$ be two families of finite dimensional subspaces parameterized by h which tends to zero. We also define

$$\begin{aligned} V_h^1 &:= \{u_h \in X_h : \ u_h = 0 \text{ on } \Gamma_w \cup \Gamma_0\}, \\ V_{0h}^1 &:= \{u_h \in X_h : \ u_h = 0 \text{ on } \Gamma_w \cup \Gamma_u \cup \Gamma_0\}, \\ Q_h^0 &:= \left\{ p_h \in S_h : \ \int_\Omega p_h \, \mathrm{d}x = 0 \ (\text{ if meas}(\Gamma_d) = 0) \right\}. \end{aligned}$$

Besides, the following assumptions are supposed to hold.

(HA1) There exists $C > 0$ such that for $0 \le m \le l$,

$$\inf_{v_h \in V_h^1} \|v_h - v\|_1 \le C h^m \|v\|_{m+1}, \qquad \forall v \in H^{m+1}(\Omega)^N \cap V^1(\Omega);$$

(HA2) There exists $C > 0$ such that for $0 \le m \le l'$,

$$\inf_{q_h \in Q_h^0} \|q_h - q\|_0 \le C h^m \|q\|_m, \quad \forall q \in H^m(\Omega) \cap Q^0(\Omega);$$

(HA3) The Ladyzhenskaya-Brezzi-Babuska inf-sup condition is verified, i.e., there exists $C > 0$, such that

$$\inf_{0 \neq q_h \in Q_h^0} \sup_{0 \neq v_h \in V_h^1} \frac{\int_\Omega q_h \operatorname{div} v_h \, \mathrm{d}x}{\|v_h\|_1 \|q_h\|_0} \ge C, \qquad V_h = V_h^1 \text{ or } V_{0h}^1.$$

The state $(y_h^n, p_h^n) \in V_h^1 \times Q_h^0$ satisfies the following fully discrete approximation of Navier–Stokes equations

$$\left\{ \begin{array}{l} \int_\Omega \left[\frac{1}{\Delta t}(y_h^n - y_h^{n-1}) \cdot v_h + 2\nu \varepsilon(y_h^n) : \varepsilon(v_h) + \mathrm{D} y_h^n \cdot y_h^{n-1} \cdot v_h - p_h^n \operatorname{div} v_h \right] \mathrm{d}x \\ \qquad\qquad = \int_{\Gamma_d} g_{2h}^n \cdot v_h \, \mathrm{d}s, \ \forall v_h \in V_{0h}^1, \text{ for } n = 1, \cdots, U, \\ \int_\Omega \operatorname{div} y_h^n q_h \, \mathrm{d}x = 0, \ \forall q \in Q_h^0, \text{ for } n = 1, \cdots, U, \\ y_h^n|_{\Gamma_u} = g_{1h}^n, \text{ for } n = 1, \cdots, U, \\ y_h^0 = y_0, \quad \text{in } \Omega, \end{array} \right. \tag{39}$$

where g_{1h}^n and g_{2h}^n are convergent approximations of the boundary conditions g_1^n and g_2^n on Γ_u and Γ_d, respectively.

The adjoint state variables $(v_h^n, q_h^n) \in V_{0h}^1 \times Q_h^0$ are solutions of the discrete adjoint system

$$\left\{ \begin{array}{l} \int_\Omega [-\frac{1}{\Delta t}(v_h^n - v_h^{n-1}) \cdot \varphi_h + 2\nu \varepsilon(v_h^{n-1}) : \varepsilon(\varphi_h) + \mathrm{D}\varphi_h \cdot y_h^n \cdot v_h^{n-1} \\ \quad + \mathrm{D} y_h^n \cdot \varphi_h \cdot v_h^{n-1} - q_h^{n-1} \operatorname{div} \varphi_h] \, \mathrm{d}x = 4\nu \chi(t) \int_\Omega \varepsilon(y_h^n) : \varepsilon(\varphi_h) \, \mathrm{d}x, \ \forall \varphi_h \in V_{0h}^1, \\ \int_\Omega \operatorname{div} v_h^{n-1} \psi_h \, \mathrm{d}x = 0, \quad \forall \psi_h \in Q_h^0, \text{ for } n = 1, \cdots, U. \\ v_h^U = 0, \qquad \text{in } \Omega. \end{array} \right.$$

(40)

The cost functional (11) are spatially discretized using the finite element space V_h^1, and time integration is performed using the trapezoidal rule which is second order accurate. The spatially and temporally integrated dissipation functions in (11) are fully discretized as

$$J_h = \nu\Delta t \sum_{n=L}^{U-1}\left(\int_\Omega |\varepsilon(y_h^n)|^2\,\mathrm{d}x + \int_\Omega |\varepsilon(y_h^{n+1})|^2\,\mathrm{d}x\right) \tag{41}$$

and the associated discrete Eulerian derivative

$$\begin{aligned}\mathrm{d}J_h(\Omega;V) = \nu\Delta t \sum_{n=0}^{U-1}\Bigg(&\int_{\Gamma_0}\left[\varepsilon(y_h^n):\varepsilon(v_h^n) - \chi(n\Delta t)|\varepsilon(y_h^n)|^2\right]V_n\,\mathrm{d}s\\ &+\int_{\Gamma_0}\left[\varepsilon(y_h^{n+1}):\varepsilon(v_h^{n+1}) - \chi((n+1)\Delta t)|\varepsilon(y_h^{n+1})|^2\right]V_n\,\mathrm{d}s\Bigg).\end{aligned}$$

5 Numerical implementation

5.1 A gradient type algorithm

For the minimization problem (10), we rather work with the unconstrained minimization problem

$$\min_{\Omega\in\mathbb{R}^2} G(\Omega) = J(\Omega) + lV(\Omega), \tag{42}$$

where $V(\Omega) := \int_\Omega \mathrm{d}x$ and l is a positive Lagrange multiplier. The Eulerian derivative of $G(\Omega)$ is

$$\mathrm{d}G(\Omega;V) = \int_{\Gamma_0} \nabla G\cdot V\,\mathrm{d}s,$$

where $\nabla G := \int_0^T [2\nu\varepsilon(y):\varepsilon(v) - 2\nu|\varepsilon(y)|^2 + l]n\,\mathrm{d}t$.

The optimization algorithm used in the present paper is a gradient type algorithm which can be summarized as follows:

(1) Choose an initial shape Ω_0, an initial step h_0 and a Lagrange multiplier l_0;

(2) Generate a computational grid that conforms to the shape of the body;

(3) Compute the state system (39);

(4) Evaluate the discrete cost functional J_h using (41);

(5) Solve the adjoint system (40);

(6) Evaluate the descent direction d_k by using (43) with $\Omega = \Omega_k$;

(7) Set $\Omega_{k+1} = (\mathrm{I} + h_k d_k)\,\Omega_k$.

In the following, we will discuss some details of the gradient type algorithm and they will make our algorithm truly efficient and effective.

5.1.1 Mesh movement

In the optimization cycle, the shape changes after each iteration. The simplest approach is to remesh after each iteration. This type is suitable for any arbitrary shapes and deformations, but it is computationally very expensive and for time–dependent flows may lead to projection errors. In the present paper a pseudo-elastic mesh movement strategy (see He, Ghattas, and Antaki (1997); E.Katamine, H.Azegami, T.Tsubata, and S.Itoh (2005); Lin, Baker, Martinelli, and et.al (2006); Tezduyar, Mittal, Ray, and et.al (1992)) is employed. The computational domain is modeled as a linear pseudo-elastic solid. The algorithm starts with a mesh of acceptable quality. The change in the location of the boundary is treated as an imposed displacement and a linear elastic boundary value problem is solved. The displacement field is taken to be the change of the internal nodes based on the given shape deformation of the solid boundary. This pseudo-elastic mesh movement strategy guarantees that the coordinates of internal nodes are smooth functions of the locations of boundary nodes. This mesh movement strategy has been proposed as procedure for solving the descent direction by

$$\int_\Omega A\varepsilon(d)\cdot\varepsilon(V)\,\mathrm{d}x = -\,\mathrm{d}G(\Omega;V). \tag{43}$$

where A is the Hooke's law defined by $A\xi = 2\mu\xi + \lambda(\mathrm{Tr}\xi)\mathrm{Id}$ with Lame moduli λ and μ. (43) indicates that the descent direction d is obtained as a displacement of a pseudo-elastic body defined in the computational domain Ω by the loading of a pseudo-external force in proportion to the negative shape gradient function $-\nabla G$. In addition, (43) can also be interpreted as a regularization of the shape gradient (see Mohammadi and Pironneau (2001), Allaire and Pantz (2006)).

5.1.2 Mesh adaptation

During the shape deformation, we utilize the a metric-based anisotropic mesh adaptation technique where the metric can be computed automatically from the Hessian of a solution.

The Hessian $\mathscr{H}_h$ of y_h can be approximated by using a recovery method, such as the Zienkiewicz-Zhu recovery procedure Zienkiewicz and Zhu (1992), the simple linear fitting Dompierre, Labb, and Guibault (2003), or the double L^2 projection

$$\mathscr{H}_h = I_{L^2}\left(\nabla(I_{L^2}(\nabla y_h))\right), \tag{44}$$

where I_{L^2} denotes the L^2 projection on the P_1 Lagrange finite element space (seeAlauzet (2003); Hecht, Pironneau, Hyaric, and Ohtsuka (2006)). Here we use (44) to get the Hessian. As it has been said in Hecht, Pironneau, Hyaric, and Ohtsuka (2006), there's no convergence proof of this method but the result is better.

5.1.3 Step size

The choice of the descent step size h_k is not an easy task. Too big, the algorithm is unstable; too small, the rate of convergence is insignificant. The classical exact line search method can be very expensive and is unnecessary to guarantee convergence in shape optimization problems. Here we use the backtracking approach Quarteroni, Sacco, and Saleri (2000). To limit the number of the required state solutions and to prevent the solver from crashing because of badly shape, it is important to provide the backtracking procedure with a good initial guess. Here we choose the initial guess h_0 so that

$$h_0 \nabla G(\Omega_k)\cdot d_k = h_{k-1}\nabla J(\Omega_{k-1})\cdot d_{k-1}.$$

5.1.4 Stopping criterion

In our algorithm, we do not choose any stopping criterion. A classical stopping criterion is to find that whether the shape gradients in some suitable norm is small enough. However, since we use the continuous shape gradients, it's hopeless for us to expect very small gradient norm because of numerical discretization errors. Instead, we fix the number of iterations. If it is too small, we can restart it with the previous final shape as the initial shape.

5.2 Numerical results

In this section we will present the results of numerical tests with the techniques described in the previous section. All the simulations presented are performed with finite element discretization in space and finite difference in time for the Navier–Stokes equations in primitive variable form. The finite element grid for the fluid region uses triangles which is generated by a Delaunay-Voronoi mesh generator (see Mohammadi and Pironneau (2001)). The finite element discretization is effected using the P_1bubble–P_1 pair of finite element spaces on a triangular mesh, i.e., we choose the following velocity space X_h and pressure space S_h:

$$
\begin{aligned}
X_h &= \{y_h \in (C^0(\bar{\Omega}))^2 : y_h|_T \in (P_{1T}^*)^2, \forall T \in \mathscr{T}_h\} \\
S_h &= \{p_h \in C^0(\bar{\Omega}) : p_h|_T \in P_1, \forall T \in \mathscr{T}_h\},
\end{aligned}
$$

where $\mathscr{T}_h$ denotes a standard finite element triangulation of Ω, P_k the space of the polynomials in two variables of degree $\leq k$ and P_{1T}^* the subspace of P_3 defined by

$$
\begin{aligned}
P_{1T}^* = \{q : q = q_1 + \lambda \phi_T,\ &\text{with } q_1 \in P_1, \lambda \in \mathbb{R} \text{ and} \\
&\phi_T \in P_3, \phi_T = 0 \text{ on } \partial T,\ \phi_T(G_T) = 1 \text{ with } G_T \text{ is the centroid of } T\}.
\end{aligned}
$$

Notice that a function like ϕ_T is usually called a bubble function.

The computations have been carried out on a home PC with Intel Pentium 4 CPU 2.8 GHz and 1GB memory.

In our computations, we choose D to be a rectangle $(-0.5, 1.5) \times (-0.5, 1.5)$ and S is to be determined in our simulations. The time interval is $[0, 3]$. The inflow velocity is assumed to be parabolic with a profile $g_1(-0.5, y) = (0.2y^2 - 0.05, 0)^T$, while at the outflow boundary Γ_d, we impose a traction-free boundary condition ($g_2 = 0$). No-slip boundary condition are imposed at all the other boundaries. We further define the admissible set

$$
\mathscr{O} := \left\{\Omega \subset \mathbb{R}^2 :\ \partial D \text{ is fixed, the area } V(\Omega) = 1.9\right\}.
$$

To begin with, we denote the reduced energy by the relative error of the cost functional: $\text{Err}_{\text{energy}} = |J_{\text{opt}}(\Omega) - J_0(\Omega)|/|J_0(\Omega)|$, where $J_{\text{opt}}(\Omega)$ and $J_0(\Omega)$ present the value of the cost functional in optimal shape and initial shape, respectively. We also denote the relative error of area $V(\Omega)$ between the area of optimal shape $V_{\text{opt}}(\Omega)$ and the target area $V_{\text{target}}(\Omega)$ by $\text{Err}_{\text{area}} = |V_{\text{opt}}(\Omega) - V_{\text{target}}(\Omega)|/V_{\text{target}}(\Omega)$.

We choose the initial shape of the body S to be a circle of center $(0, 0)$ with radius $r = 0.3$. The characteristic time interval for cost functional is $[t_L, t_U] = [1, 3]$ and we set the time step $\Delta t = 0.1$.

We present results for different Reynolds numbers $\text{Re} = 40, 100, 200, 300, 400$ defined by $\text{Re} = 2r|y_{\text{m}}|/\nu$, where y_{m} is the maximum velocity at the inflow Γ_u. The finite element meshes used for the calculations at $\text{Re} = 40$ have been shown in Figure 1 which consists of 1796 elements with 988 vertices.

Figure 2—Figure 7 give several snapshots in time of horizontal velocity streamlines corresponding to the initial shape and optimal shape with Reynolds numbers $\text{Re} = 100, 200, 400$, respectively. Note that the optimizer has found a symmetric optimal shape, despite the fact that symmetry has not been imposed as a constraint in the

problem, and the unstructured mesh (see Figure 1) is not symmetric. We also find that the center of balance of the body is moved backward.

In Figure 8–Figure 10, time histories of the viscous dissipation energy function $\Phi(y) = 2\nu \int_\Omega |\varepsilon(y)|^2 \, dx$ are computed with initial shape and optimal shape for Reynolds numbers $\mathrm{Re} = 100, 200, 400$, respectively.

Optimization histories for various Reynolds numbers are plotted in Figure 11. In Table 1, we present the results obtained for the fixed reduced energy $\mathrm{Err}_{\mathrm{energy}} = 74\%$. It is obvious that when Re increases, the total dissipated energy for the optimal cannula decreases and the corresponding computational cost raises. The area of the optimal solid body is located in the range $(1.896, 1.908)$. The large CPU time is due to the need for time–accurate integration and the computation of flow systems at each time step.

Conclusion

In this work, the viscous dissipation energy minimization problem of a solid body located in the time–dependent incompressible Navier–Stokes flow is presented. The volume of the target body is kept constant. The shape gradient which is obtained by the function space parametrization technique is used to obtain the optimal shape of the body. The flow systems are discretized in space using a P_1bubble–P_1 finite element formulation, and a Crank–Nicholson scheme is used for integration in time. We have proved the effectiveness of the proposed gradient type algorithm with mesh adaptation and mesh movement strategies and compared the results for different Reynolds numbers. Further study is on numerical simulation for very large Reynolds numbers.

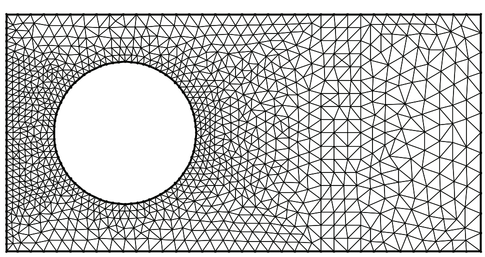

Figure 1: The finite element mesh for the initial shape (Re=40).

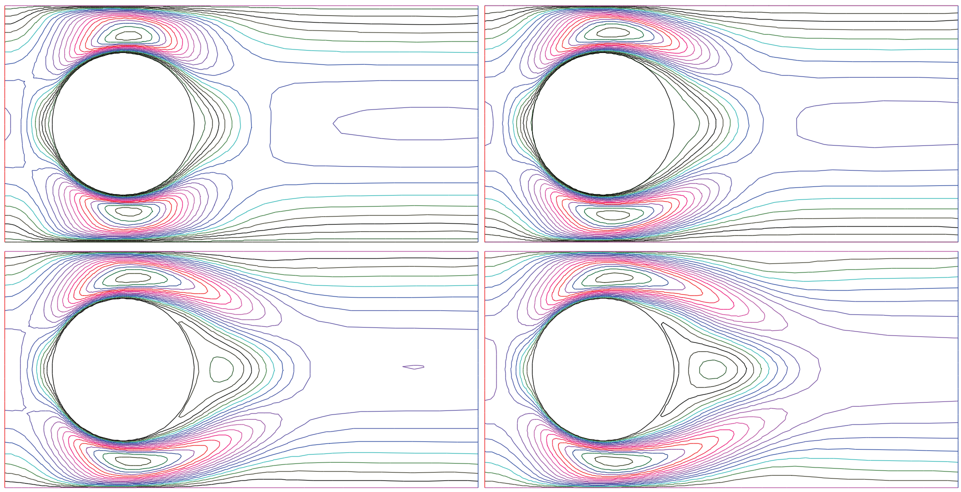

Figure 2: Horizontal velocity at $t = 0.4$ (upper left), 1.2 (upper right), 2 (bottom left), 2.8 (bottom right) for the initial shape (Re=100).

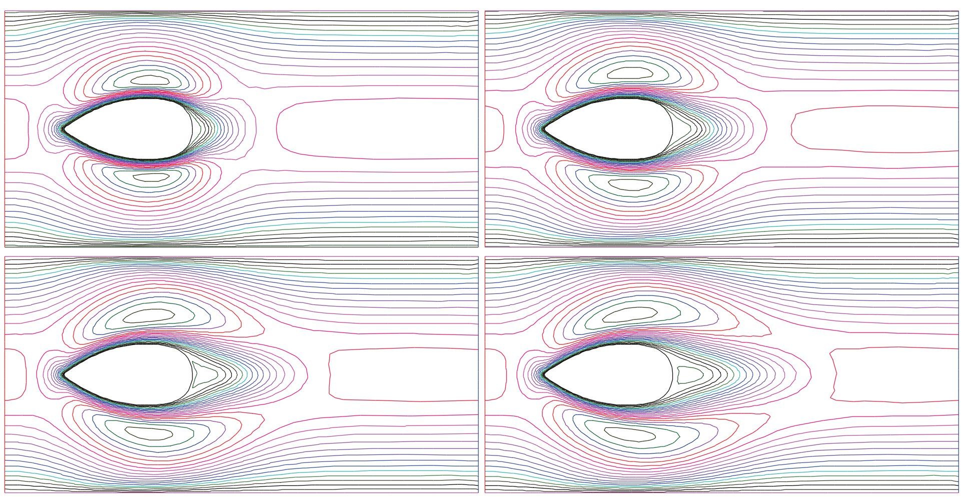

Figure 3: Horizontal velocity at $t = 0.4$ (upper left), 1.2 (upper right), 2 (bottom left), 2.8 (bottom right) for the optimal shape (Re=100).

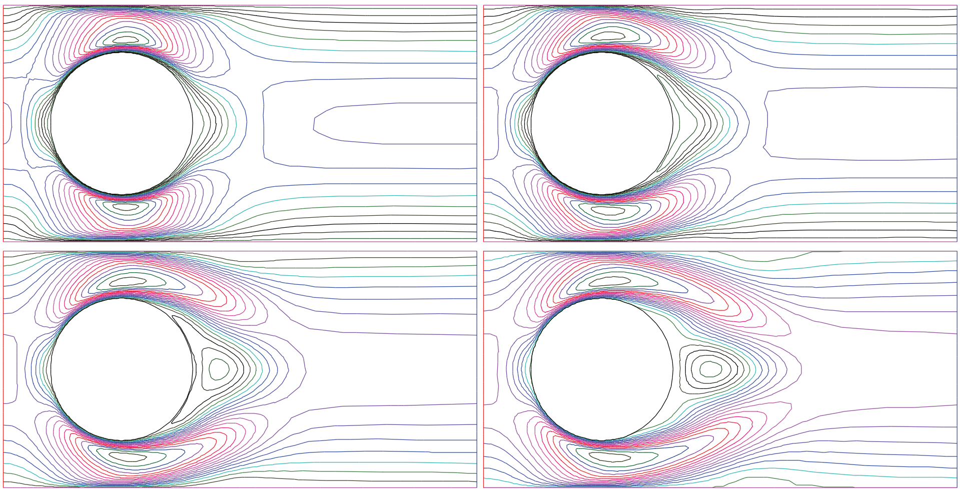

Figure 4: Horizontal velocity at $t = 0.4$ (upper left), 1.2 (upper right), 2 (bottom left), 2.8 (bottom right) for the initial shape (Re=200).

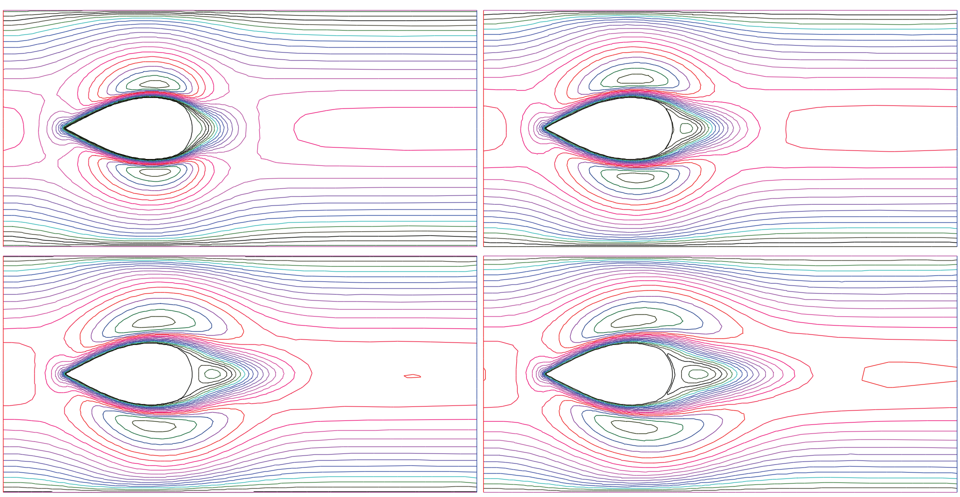

Figure 5: Horizontal velocity at $t = 0.4$ (upper left), 1.2 (upper right), 2 (bottom left), 2.8 (bottom right) for the optimal shape (Re=200).

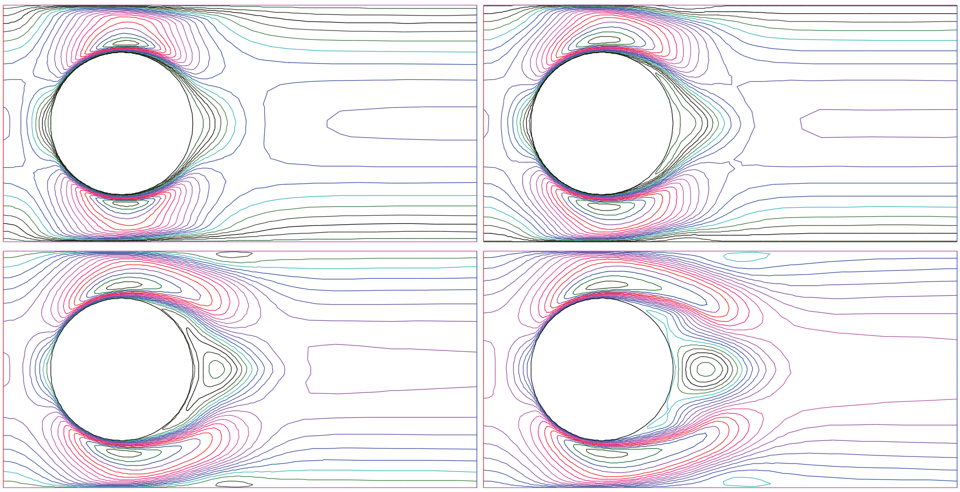

Figure 6: Horizontal velocity at $t = 0.4$ (upper left), 1.2 (upper right), 2 (bottom left), 2.8 (bottom right) for the initial shape (Re=400).

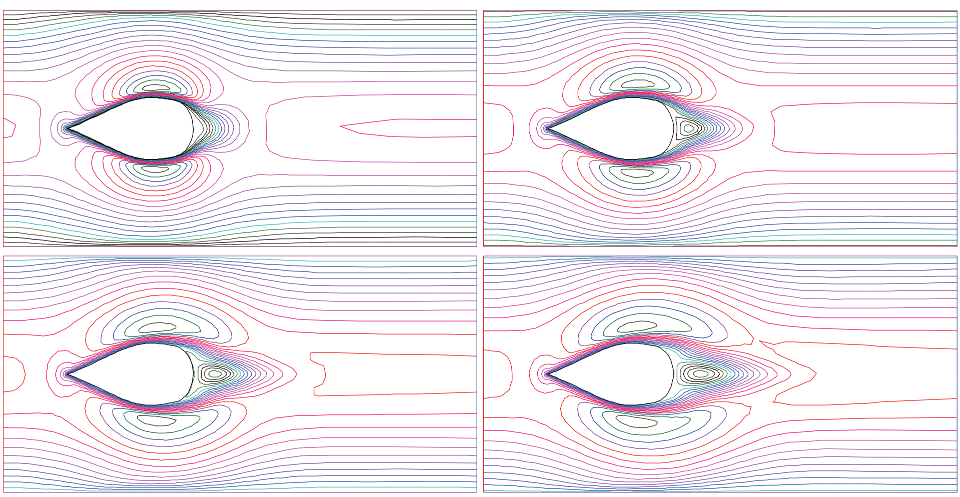

Figure 7: Horizontal velocity at $t = 0.4$ (upper left), 1.2 (upper right), 2 (bottom left), 2.8 (bottom right) for the optimal shape (Re=400).

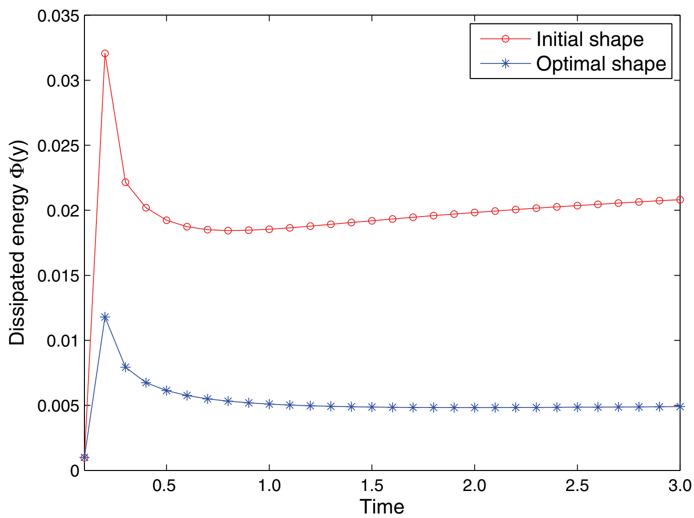

Figure 8: Time history of the dissipation function (Re=100).

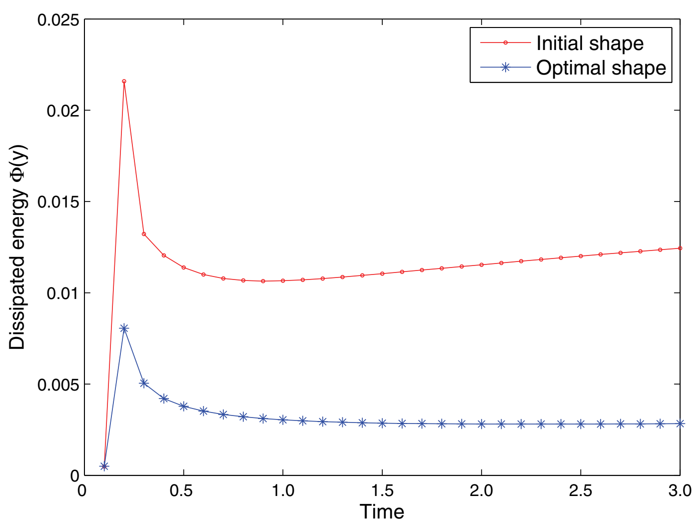

Figure 9: Time history of the dissipation function (Re=200).

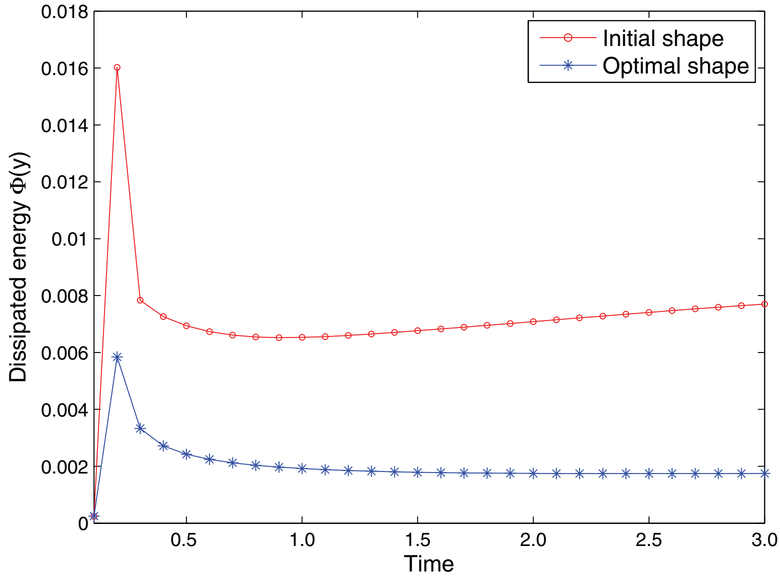

Figure 10: Time history of the dissipation function (Re=400).

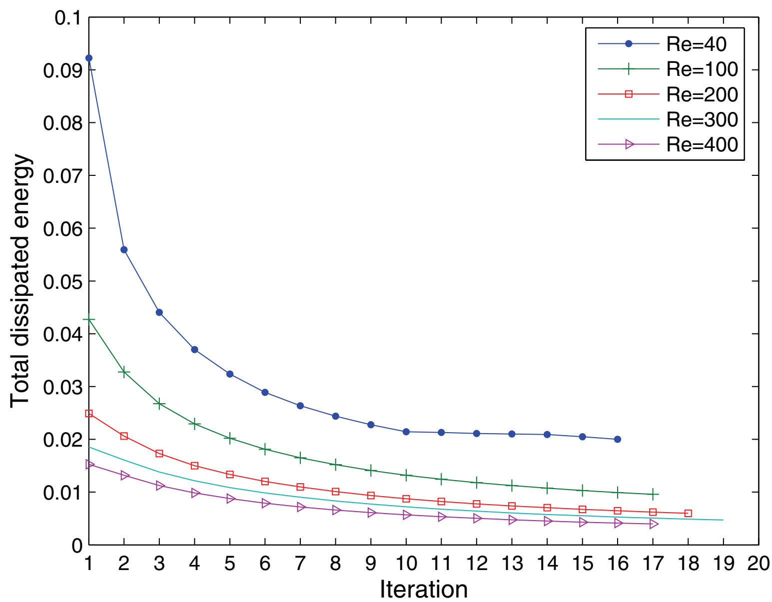

Figure 11: Cost functional as a function of number of optimization iterations for various Reynolds numbers.

Table 1: The numbers of iterations, the reduced total dissipated energy $\mathrm{Err}_{\mathrm{energy}}$, CPU times, the optimal areas for various Reynolds numbers.

$\mathrm{Err}_{\mathrm{energy}}$	Re	Iterations	Energy	$V_{\mathrm{opt}}(\Omega)$	$\mathrm{Err}_{\mathrm{area}}$	CPU time
74%	40	7	0.0243893	1.89666	1.76×10^{-3}	2211.86s
74%	100	12	0.0112406	1.89655	1.82×10^{-3}	3692.70s
74%	200	15	0.00646516	1.90306	1.61×10^{-3}	4976.91s
74%	300	16	0.00606068	1.90368	1.94×10^{-3}	5319.58s
74%	400	17	0.00396328	1.90794	4.18×10^{-3}	5512.53s

References

Abraham, F.; Behr, M.; Heinkenschloss, M. (2005): Shape optimization in unsteady blood flow: a numerical study of non-Newtonian effects. *Computer Methods in Biomechanics and Biomedical Engineering*, vol. 8, pp. 201–212.

Alauzet, F. (2003): *Adaptation de maillage anisotrope en trois dimensions. Application aux simulations instationnaire en Mecanique des Fluides*. PhD thesis, Universit des Sciences et Techniques du Languedoc, 2003.

Allaire, G.; Pantz, O. (2006): Structural optimization with freefem plus. *Structural and Multidisciplinary Optimization*, vol. 32, no. 3, pp. 173–181.

Bello, J.; Fernandez-Cara, E.; Lemoine, J.; Simon, J. (1997): The differentiability of the drag with respect to the variations of a lipschitz domain in a Navier-Stokes flow. *SIAM Journal of Control and Optimization*, vol. 35, no. 2, pp. 626–640.

Bello, J.; Fernandez-Cara, E.; Simon, J. (1992): Optimal shape design for navier-stokes flow. In Kall, P.(Ed): *System modelling and optimization*, no. 180 in Lecture Notes in Control and Inform. Sci., pp. 481–489. Springer.

Bello, J.; Fernandez-Cara, E.; Simon, J. (1992): The variation of the drag with respect to the domain in Navier-Stokes flow. In *Optimization, optimal control, partial differential equations*, no. 107 in International Series of Numerical Mathematics, pp. 287–296. Birkhauser.

Céa, J. (1981): Problems of shape optimal design. In E.J.Haug; J.Céa(Eds): *Optimization of Distributed Parameter Structures*, volume II, pp. 1005–1048. Sijthoff and Noordhoff, Alphen aan denRijn.

Correa, R.; Seeger, A. (1985): Directional derivative of a minmax function. *Nonlinear Analysis, Theory Methods and Applications*, vol. 9, pp. 13–22.

Delfour, M. C.; Zolesio, J.-P. (2002): *Shapes and Geometries: Analysis, Differential Calculus, and Optimization*. Advance in Design and Control. SIAM.

Dompierre, J.; Labb, P.; Guibault, F. (2003): Controlling approximation error. In *Second M.I.T Conference on Computational Fluid and Solid Mechanics*, pp. 1929–1932. Cambridge, Elsevier.

E.Katamine; H.Azegami; T.Tsubata; S.Itoh (2005): Solution to shape optimization problems of viscous flow fields. *International Journal of Computational Fluid Dynamics*, vol. 19, no. 1, pp. 45–51.

E.Katamine; H.Azegami; Y.Matsuura (2003): Solution to shape identification problem of unsteady heat conduction fields. *Heat Transfer-Asian Research*, vol. 32, no. 3, pp. 212–226.

Gao, Z.; Ma, Y. (2006): Shape sensitivity analysis for a Robin problem via minimax differentiability. *Applied Mathematics and Computation*, vol. 181, no. 2, pp. 1090–1105.

Gao, Z.; Ma, Y. (2008): Shape gradient of the dissipated energy functional in shape optimization for the viscous incompressible flow. *Applied Numerical Mathematics*, vol. 58, no. 11, pp. 1720–1741.

Gao, Z.; Ma, Y.; Zhuang, H. (2008): Optimal shape design for stokes flow via minimax differentiability. *Mathematical and Computer Modelling*, vol. 48, no. 3-4, pp. 429–446.

Gao, Z.; Ma, Y.; Zhuang, H. (2008): Shape optimization for Navier–Stokes flow. *Inverse Problems in Science and Engineering*, vol. 16, no. 5, pp. 583–616.

Gunzburger, M. D. (2003): *Perspectives in flow control and optimization*. SIAM, Philadelphia.

Hadamard, J. (1907): Mémoire sur le problème d'analyse relatif à l'équilibre des plaques élastiques encastrées. In *Mémoire des savants étrangers*, no. 33.

He, B.; Ghattas, O.; Antaki, J. (1997): Computational strategies for shape optimization of time-dependent Navier-Stokes flows. Technical Report CMU-CML-97-102, Computational Mechanics Laboratory, Carnegie Mellon University, Pittsburgh, 1997.

Hecht, F.; Pironneau, O.; Hyaric, A. L.; Ohtsuka, K. (2006): Freefem++ manual. http://www.freefem.org, 2006.

Lin, P. T.; Baker, T. J.; Martinelli, L.; et.al (2006): Two-dimensional implicit time-dependent calculations on adaptive unstructured meshes with time evolving boundaries. *Int. J. Numer. Meth. Fluids*, vol. 50, pp. 199–218.

Mohammadi, B.; Pironneau, O. (2001): *Applied Shape optimization for fluids*. Clardendon press, Oxford.

Murat, F.; Simon, J. (1974): Quelques resultats sur le controle par un domaine geometrique. Technical Report 74003, Universite Paris VI., 1974. Rapport du L.A. 189.

Pironneau, O. (1984): *Optimal Shape Design for Elliptic systems*. Springer, Berlin.

Pironneau, O. (1988): Optimal shape design by local boundary variations. In B.Kawohl; O.Pironneau; L.Tartar(Eds): *Optimal shape design*. Springer. Lectures given at the joint C.I.M.

Quarteroni, A.; Sacco, R.; Saleri, F. (2000): *Numerical mathematics*, volume 37 of *TAM*. Springer-Verlag, New York.

Quarteroni, A.; Valli, A. (1994): *Numerical approximation of partial differential equations*. Springer-Verlag, New York.

Simon, J. (1980): Differentiation with respect to the domain in boundary value problems. *Numer. Funct. Anal.Optim.*, vol. 2, pp. 649–687.

Sokolowski, J.; Zolesio, J.-P. (1992): *Introduction to Shape Optimization: Shape Sensitivity Analysis*. Springer-Verlag.

Srinath, D. N.; Mittal, S. (2007): A stabilized finite element method for shape optimization in low Reynolds number flows. *International Journal for Numerical Methods in Fluids*, vol. 54, pp. 1451–1471.

Tezduyar, T. E.; Mittal, S.; Ray, S. E.; et.al (1992): Incompressible flow computations with stabilized bilinear equal-order-interpolation velocity-pressure elements. *Computer Methods in Applied Mechanics and Engineering*, vol. 95, pp. 221–242.

Yagi, H.; Kawahara, M. (2005): Shape optimization of a body located in low reynolds number flow. *International Journal for Numerical Methods in Fluids*, vol. 48, pp. 819–833.

Yagi, H.; Kawahara, M. (2007): Optimal shape determination of a body located in incompressible viscous fluid flow. *Computer Methods in Applied Mechanics and Engineering*, vol. 196, no. 49-52, pp. 5084–5091.

Zienkiewicz, O. C.; Zhu, J. Z. (1992): The superconvergent patch recovery and a posteriori error estimates. Part I: the recovery technique. *Int. J. Numer. Meth. Engng*, vol. 33, no. 7, pp. 1331–1364.

Zolesio, J.-P. (1979): *Identification de domaines par déformation*. PhD thesis, Université de Nice, 1979.